SHM-BASED PRACTICAL SAFETY EVALUATION AND VIBRATION CONTROL MODEL FOR STEEL PIPES

Sang Geun BAE[1], Jewoo CHOI[1], Deok Shin KANG[2], Taehoon HONG[1],
Dong-Eun LEE[3], Hyo Seon PARK[1*]

[1]Department of Architectural Engineering, Yonsei University, Seoul, Korea
[2]Hyundai Engineering & Construction, Seoul, Korea
[3]School of Architecture, Civil Engineering, Environment, and Energy,
Kyungpook National University, Daegu, Korea

Abstract. Unexpected damages or failures of steel pipes in refineries cause significant disruption to economic activity. While research has been conducted on the prevention of damage to steel pipes, no systematic methods or practical techniques for monitoring of vibrations to estimate the state of pipeline system have been reported. In this study, vibration safety evaluation model consisting of design – evaluation – control steps was developed to measure and control the vibration level during operation of the piping system of an oil refinery. The measurement location was designed by examining the structure of the pipe, and the vibration level measured at each location was compared with the allowable vibration level. Subsequently, two types of vibration reduction measures, namely, dynamic absorbers and viscous dampers, were introduced to reduce the vibration level. The effect of the application of the monitoring system was evaluated by comparing the vibration levels of the steel pipes before and after the application of the dynamic absorbers and viscous dampers. The vibrations of steel pipes in the oil refinery during operation decreased by over 50%. Upon applying the dynamic absorbers and viscous dampers, the responses of the frequency component also exhibited local and global reductions of approximately 50–80%.

Keywords: monitoring system, measurement, steel pipe, oil refinery.

Introduction

The rupturing of steel pipes in refineries, which result in explosions and environmental pollution, occur continually worldwide. The brittle failure of pipes in a plant instantaneously releases a large amount of high-temperature and high-pressure fluid and severely affects various devices and components around the pipes (Gabbianelli et al., 2023; Iqbala et al., 2017; Miranda et al., 2010; Chock, 2006; Whittaker & Soong, 2003; Taghavi & Miranda, 2003). Furthermore, global seismic events have caused significant economic losses to industrial structures and their components over the pastseveral decades (Ozdemir et al., 2010; González et al., 2010; Brunesi et al., 2015; Vela & Nascimbene, 2019; Gabbianelli et al., 2022). The damage attributed to pipe vibrations in developed countries is estimated annually at US$ 10 billion (Hussein & Al-Waily, 2019). Therefore, research on the prevention of damage to steel pipes in refineries caused by the vibrations of fluid pipes

is valuable in terms of securing structural safety and economic aspects (Parvizsedghy et al., 2015; Sun et al., 2013).

Senouci et al. (2014) used regression analysis and artificial neural network models to aid decision-makers predict the failure occurrence of pipelines. These two models have been successfully applied to predicting pipeline failures caused by mechanical, operational, corrosion, third-party, and natural hazards. Kabir et al. (2016) developed a safety assessment model for oil and gas pipeline failures by incorporating fuzzy logic into a Bayesian belief network. Construction defects, overloads, mechanical damage, bad installation, and poor quality of workers were identified as the most significant causes of oil and gas pipeline failures. Ariaratnam and Namachchivaya (1986) proposed an analytical method for the stability of analysis of pipe systems. Olson and Jamison (1997) used finite element formulas for four types of pipe-end conditions to analyze calculated

*Corresponding author. E-mail: *hspark@yonsei.ac.kr*

and theoretical results and compare them. Zhang et al. (2001) proposed a finite element method to perform a dynamic analysis of initially tensioned thin-walled orthotropic cylindrical tubes conveying a normal flow of fluid, and they validated it via comparison with the obtained natural frequencies. Seo et al. (2005) used a finite element method to formulate cylindrical shells that convey fluids at a uniform velocity; they observed that as the velocity increases, the rigidity decreases and the damping increases, thereby decreasing the natural frequency and peak.

Tan et al. (2019) designed spring-steel and simple-pendulum pounding tuned mass dampers (PTMDs) to mitigate the vibration of a suspended piping system without fluids. The two PTMDs were compared with a regular tuned mass damper (TMD) in free vibration and forced vibration tests. The PTMDs exhibited faster vibration suppression effects than the TMD for both vibration types. However, the experiments were conducted using the amplitude for a specific domain and did not consider the additional mass of the liquid.

Many studies have analyzed the static and dynamic behaviors of the structural vibrations of piping systems in various aspects. The free vibration of regular structures with no fluid is determined using only the mass and rigidity for a specified structure; however, the dynamic behavior of a pipe that conveys a fluid is complex to analyze because the natural frequency decreases as an axial force is applied and the force increases (Jweeg & Ntayeesh, 2015). To investigate flow-induced vibration (FIV), Miwa et al. (2015) divided structural and fluid dynamics problems and analyzed the two-phase FIV; they identified the churn of the fluid and slug generated inside as the main cause of the vibration. A method for minimizing the generation of slugs was proposed to resolve this issue; it increases the natural frequency of the pipe structure beyond the vibration range of the two-phase fluid through rigid solid fixtures or supports to avoid resonance and rapid direction changes.

Generally, the reliability of the vibration analysis of piping systems in the design phase is low, and flow analysis is time-consuming because it is affected by numerous field conditions (Mossa et al., 2018). To evaluate and control the vibration level of structures in use or under construction, researchers have applied structural health monitoring (SHM) technology to the field measurements of vibrations (Zhang et al., 2021; Zhou et al., 2018; Amezquita-Sanchez & Adeli, 2016; Yildirim et al., 2013; Xiao et al., 2021; Sepehry et al., 2020; Riveiro et al., 2016; Wang et al., 2006). Because safety and vibration can be evaluated using the identified modal parameters from measurement data, various SHM technologies have been developed (Wang et al., 2021; Yun et al., 2021; Kim et al., 2017; Park & Oh, 2018).

However, research on the evaluation of the structural condition monitoring during operation of pipelines is still insufficient, and the degree of the external shock detection system is suggested through analysis and monitoring considering various aspects of the pipe structure. This paper proposes a steel pipe vibration control model consisting of three stages: design, evaluation, and control, for pipelines that are already installed and operating.

In the design stage, we conducted an investigation of the pipeline and proposed measurement locations. The evaluation stage involved measuring the vibration of the pipeline and searching for sections that exceeded the specified threshold. The measured vibration level is compared with the allowable vibration level based on the American Society of Mechanical Engineers [ASME] OM Part 3 standards (ASME, 2001). Finally, in the Mitigation stage, we proposed appropriate vibration reduction measures. Based on the comparison results of the measured and allowable vibrations, two types of vibration reduction measures are considered to reduce the vibration level: dynamic absorbers and viscous dampers. The monitoring system was applied to control the vibration level of the steel pipes in a refinery during operation. The effect of applying the monitoring system was evaluated by comparing the vibration levels of steel pipes in the refinery before and after the application of the monitoring system.

1. Monitoring system for vibration of steel pipes in refineries

In this study, a monitoring system using accelerometers was developed to evaluate the vibration level and maximum stress of pipes in an oil pipeline in the field. The monitoring system was used to evaluate the vibration levels of pipes before and after the application of dampers and absorbers to reduce the vibration levels.

1.1. Piping system

Figure 1 shows the steel pipes in the pipelines of an oil factory in the field to be monitored. The pipes were U-bend and Z-bend pipes with diameters of 10 and 24 inches, respectively, and the support conditions were all fixed.

The Z-bend consisting of three sections was denoted by Z1, Z2, and Z3, and the location and end condition of the Support U-bend (SU) and Support-Z bend (SZ) is shown in Figure 1a. The figure is drawn relatively enlarged to explain the U-bend structure. A schematic of the pipes classified by pipe size is presented in Figure 1b by rotating the pipes in Figure 1a by 90° in the counterclockwise direction. To control the vibration levels of the pipe in the pipeline, we measured the vibration of pipes at the sections at which vibration occurred. The pipe sections shown in Figure 1 were fabricated from A106-B steel with a yield strength of 240 MPa.

As shown in Figure 1, the pipe sizes were primarily classified into two parts: upper (colored in red) and lower (colored in blue) pipes. The nominal pipe sizes of the lower and upper pipes were 10 and 24 inches, respectively. On-site photographs of the pipes are shown in Figure 2.
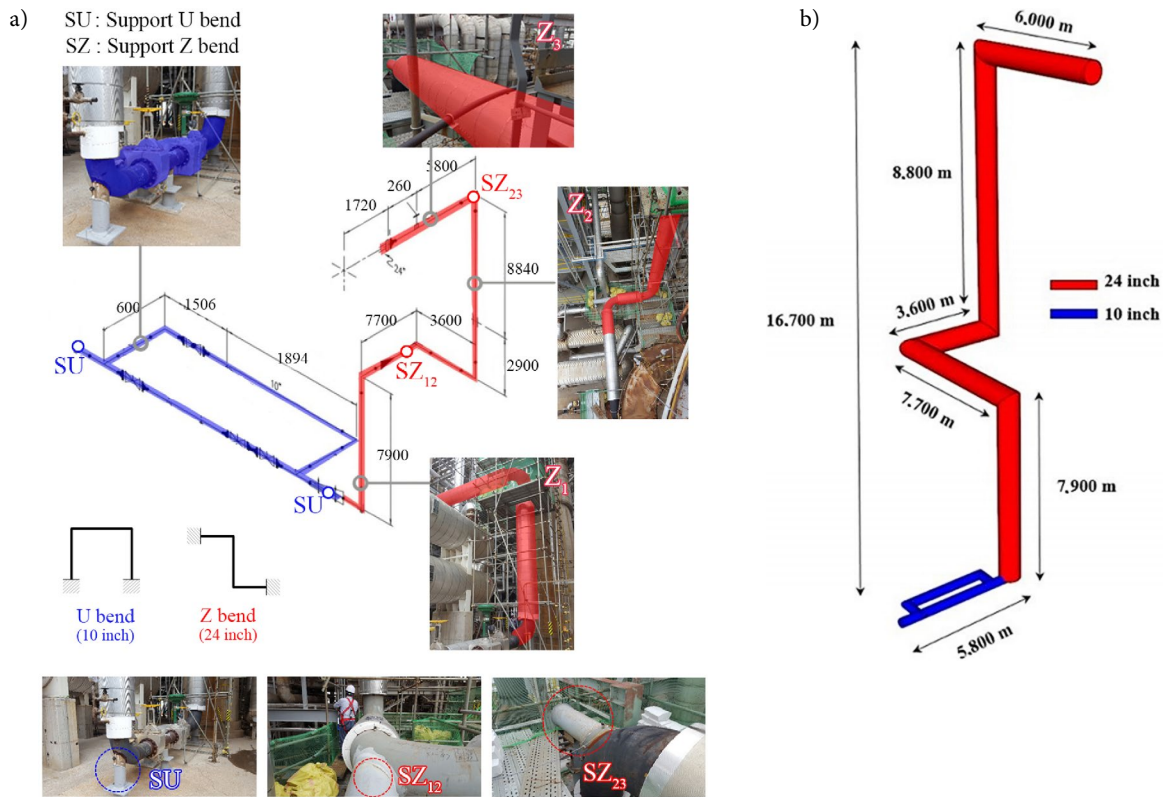
Figure 1. Steel pipes in oil pipeline to be monitored: a – Bend and support type of steel pipes;
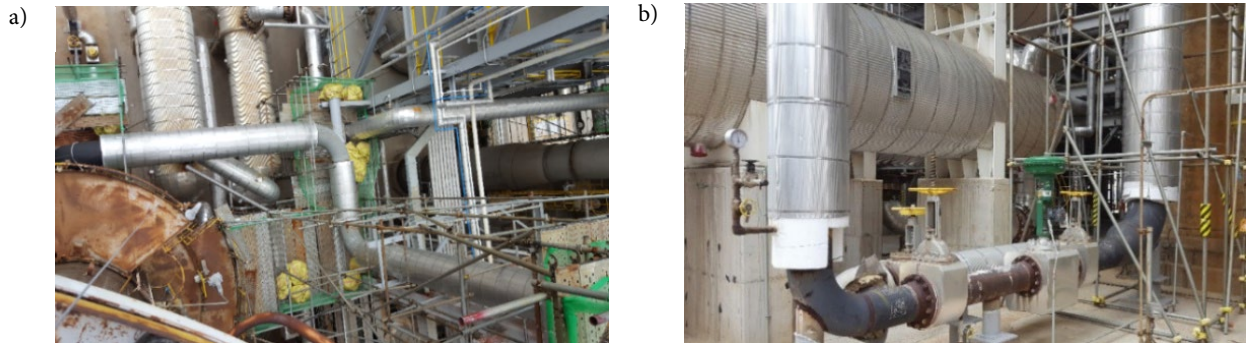b – Classification of pipes by the size of section

Figure 2. Photos of upper and lower pipes in pipelines of oil factory: a – 24 inch pipes in upper part;
b – 10 inch pipes in lower par

1.2. Measurement system for vibration of pipes

Figure 3 illustrates the practical field measurement system used in this study. The acceleration data obtained using a Wilcoxon 993A 3-axial accelerometer were the signals received and converted from a SIEMENS SCADAS XS data logger. The hardware used in this study was a Lenovo T460 laptop, and the signal analysis software used was LMS Test.Lab.

1.3. Measurement locations

Figure 4 shows the on-site photographs of the accelerometers attached to the surface of the pipes; as shown in the figure, vibrations were measured at 11 points based on the pipe branching points, vertical and horizontal elbows, and supports.

2. Evaluation of vibration level of pipes

Simplified methods for evaluating the vibration level of steel pipes in refineries include the displacement and the velocity methods, of which the velocity method was used in this study. Depending on the level of vibration of the pipes, we can determine whether to perform additional analysis to mitigate the vibration level of pipes.

2.1. Allowable velocity baseline of pipes according to ASME OM part 3

To determine the vibration level of the pipes, the allowable vibration level using the velocity of the pipes of the oil plant can be expressed as V_{allow} by ASME OM part3 (ASME, 2001):

$$V_{allow} = \frac{C_1 C_4}{C_3 C_5} \frac{\beta(S_{el})}{\alpha C_2 K_2} \quad \text{(where } \beta = 1.34 \text{ mm/s)}, \quad (1)$$

where V_{allow} is the allowable peak velocity (mm/s), and C_1 is a correction factor for compensating for the effect of concentrated weights, such as valves, along the characteristic span of the pipe (Xue et al., 2007). For straight beams, L-bends, U-bends, and Z-bends, if the concentrated weight is less than 17 times the span weight, a conservative value of 0.15 can be used for C_1 for screening.

$C_2 K_2$ is the stress index defined by the ASME BPV Code (ASME, 2010). In most steel pipes in refineries, s $C_2 K_2$ has a value of less than or equal to 4, and is calculated as follows (Xue et al., 2007):

$$C_2 K_2 = \frac{0.9}{(t_n R / r^2)^{2/3}}, \quad (2)$$

where t_n is thickness of matching pipe (in), R is radius to center line of curvature for elbows or smooth bends (in), and r is mean radius of matching pipe (in) (Figure 5).
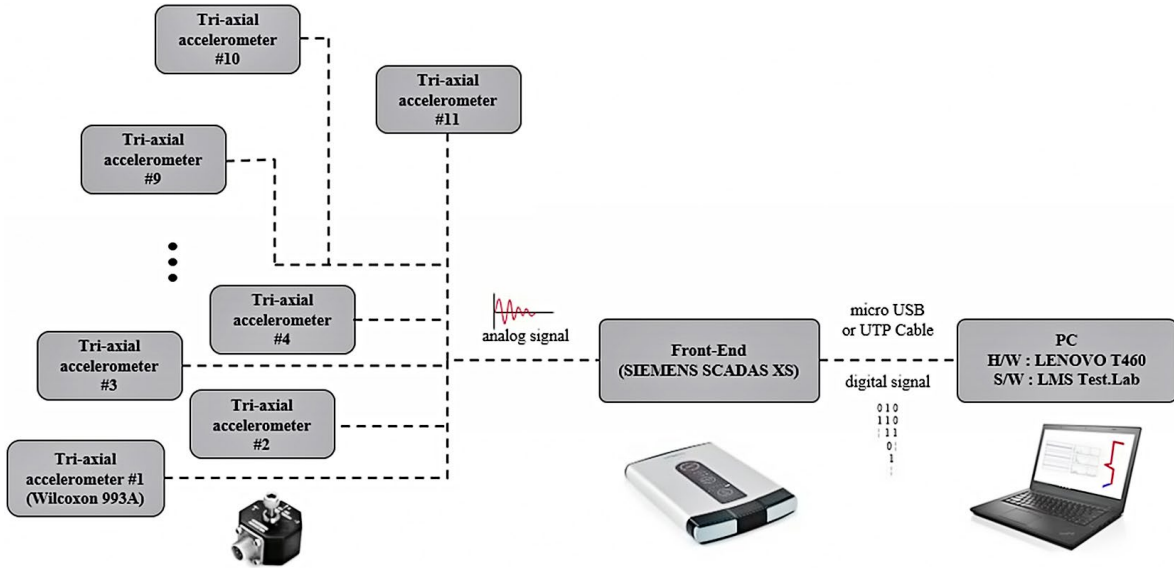

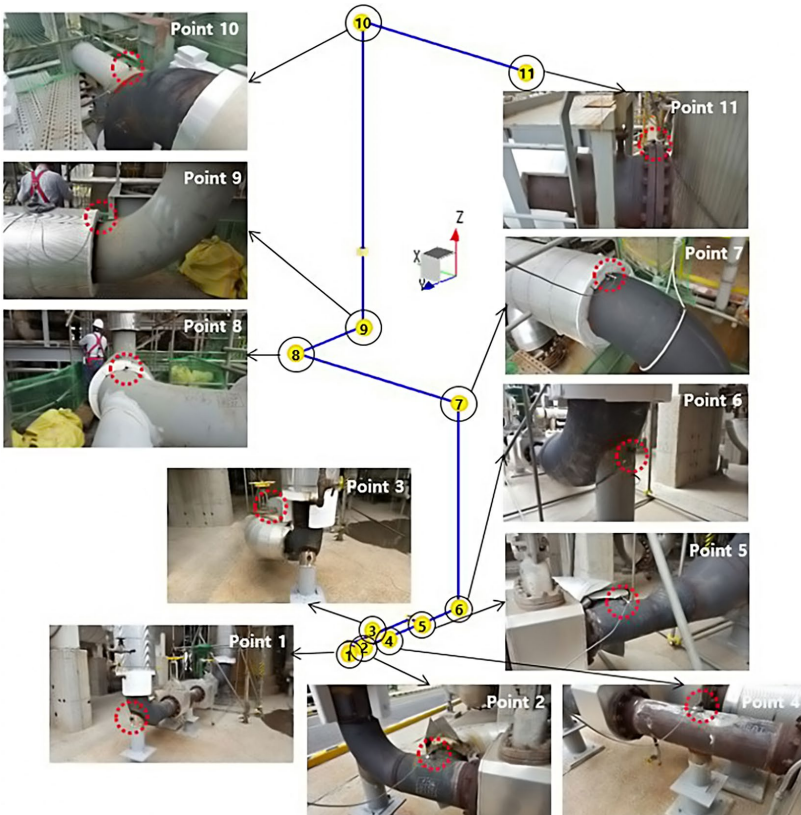Figure 3. Composition of the vibration measurement system

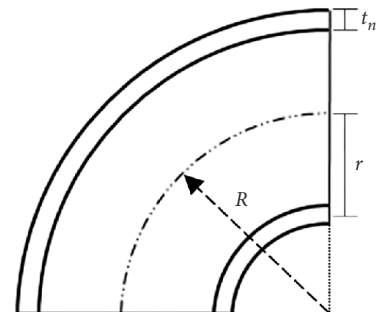Figure 4. Locations for vibration measurements on the pipes

Figure 5. Dimensions of pipes for the correction factor $C_2 K_2$

C_3 is the correction factor for the thermal insulator and pipe contents and is calculated as follows:

$$C_3 = \sqrt{1 + \frac{W_f}{W} + \frac{W_{Ins}}{W}}, \qquad (3)$$

where W is the weight of the pipe per unit length (kg/m), W_f is the weight of the pipe content per unit length (kg/m), and W_{Ins} is the weight of the thermal insulation per unit length (kg/m). C_4 is a correction factor for the boundary condition and span configuration of the pipe. Span configurations can be classified as straight, Z-bends, and U-bends. The straight span has a value of 1.0 when the boundary condition is fixed ends and 1.33 when the boundary condition is cantilever and simply supported. When the configuration is a Z- or U-bend, the correction factor C_4 is 0.74 or 0.83, respectively (ASME, 2012). C_5 is the same as the ratio of the first natural frequency (F_n) to the measured frequency (F_m), and it is the correction factor for explaining the off-resonance forced vibration. If the ratio is larger than 2.0, C_5 is not defined; if it is less than 1.0, C_5 is 1.0.

For a normal state vibration, the calculated maximum alternating stress intensity (S_{alt}) is defined by

$$S_{alt} = \frac{C_2 K_2}{Z} M \le \frac{S_{el}}{\alpha}, \qquad (4)$$

where M is the maximum zero to peak dynamic moment loading due to vibration, Z is the sectional modulus of the pipe, S_{el} is 0.8SA, and SA is the alternating stress at 10^6 cycles in psi (MPa). α is the allowable stress reduction factor, which is defined as 1.3 or 1.0 depending on the pipe material.

2.2. Application of vibration velocity baseline according to correction factors

Table 1 shows the method of calculating vibration velocity based on the correction factor that uses a conservative baseline by classifying the pipe size into 10 and 24 inches. The baseline velocity range calculated using Eqn (1) with the variables of Table 1 is 14.8–32.6 mm/s for 10-inch pipes, and 14.8 mm/s is used as the conservative baseline; it is 17.2–34.0 mm/s for 24-inch pipes, for which 17.2 mm/s is used as the conservative baseline.

The acceleration is measured at each point using the measurement system described in Section 2.2. The accurate velocity values are obtained through integration by processing acceleration data using a 1.5 Hz high-pass filter to suppress variations in the low-frequency range and to remove constant terms from the initial conditions (Zhu et al., 2020; Guo et al., 2022). The vibration levels at each measurement point are expressed as velocity values in the x, y, and z directions in Table 2. As shown in Table 2, the results of the pipe vibration evaluation based on the ASME screening criteria show that the baseline was exceeded at points 5 and 7–10, indicating that the baseline for vertical pipes is exceeded mostly in the vertical and horizontal directions.

Figure 6a depicts the result of Fast Fourier transform (FFT) on the acceleration data measured at Node 7, confirming that the main vibration mode was at 3.25 Hz. The RMS value of the FFT amplitude was employed to intuitively understand the magnitude of the attenuated energy both before and after attaching the vibration reduction device (Escaler et al., 2006; Valentín et al., 2019; Al-Obaidi, 2020; Bhandari & Jotautienė, 2022). To verify whether the

Table 1. Variables according to the pipe section size

| Pipe size	C_1	$C_2 K_2$	C_3	C_4	S_{el}/α
10 inch	0.28 (5 times of average concentrated mass) 0.15 (17 times of conservative baseline)	$R = 381$ mm $r = 131.9$ mm $t_n = 9.271$ mm	Pipe: 7833.0 kg/m^3 Fluid: 558.3 kg/m^3 Insulation: 208.2 kg/m^3	0.83 (U-bend)	53
24 inch	0.28 (five times the average concentrated mass) 0.15 (17 times the conservative baseline)	$R = 914.4$ mm $r = 300.0$ mm $t_n = 9.525$ mm	Pipe: 7833.0 kg/m^3 Fluid: 19.06 kg/m^3 Insulation: 208.2 kg/m^3	0.74 (Z-bend)	53

a)

b)
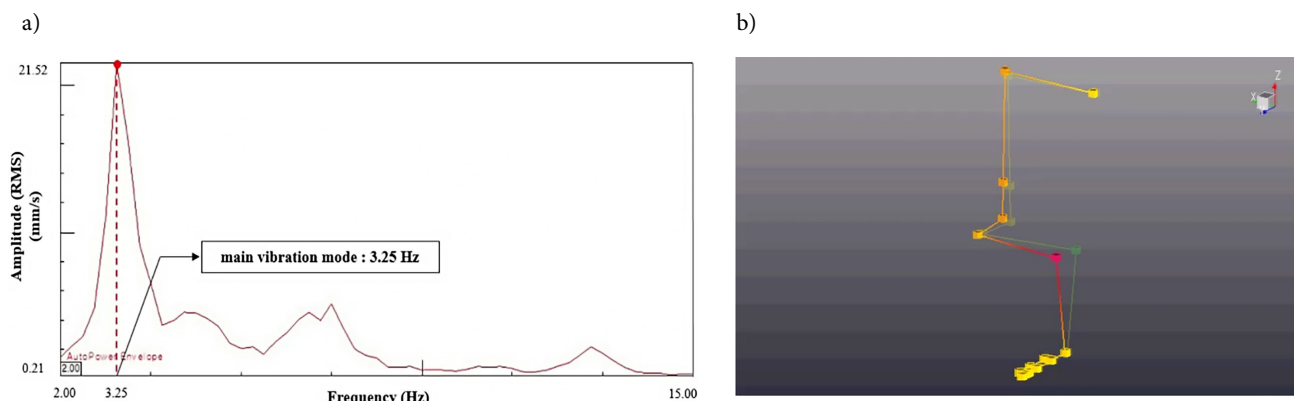
Figure 6. Vibration deformation shape through operational deformed shape (ODS) analysis: a – FFT plot of the piping system; b – Deformed shape (3.25 Hz)

searched frequency was the natural frequency of the pipeline, we confirmed through the finite element analysis that the first mode frequency appeared the same at 3.25 Hz. Figure 6b shows the deformed shape of the entire pipe in the corresponding mode (3.25 Hz). The displacement value increased (from the value denoted by yellow to that denoted by red), and the largest displacement occurred in the horizontal direction (y axis) at point 7 (marked in red). Therefore, vibration levels must be reduced by installing appropriate viscous dampers and dynamic absorbers.

3. Application of dampers and absorbers

Depending on the source of the vibration, various devices are used to reduce the vibration levels for each pipe according to the force. The oil pipe system in this study vi-

brated in the low-frequency region because of the natural frequency and mode shape of the pipe system due to the random load caused by the fluid turbulence. Generally, vibration reduction measures for pipes are based on the principle of applying a reduction measure at the maximum response point. Consequently, a behavioral pattern analysis of the main vibration components of the pipe vibration response is crucial. The reduction measures included damping reinforcement and rigidity reinforcement. However, in this study, the rigidity reinforcement method that controls vibrations by adding and reinforcing supports at other parts in addition to existing supports was excluded because the stress concentration phenomenon owing to thermal deformation can occur in steel pipes in refineries. The masses of the dynamic absorber and viscous damper can add rigidity to the pipe. However, the

Table 2. Vibration level evaluated at each measurement point

Measurement point (Node no.)		Peak velocity (mm/s)	Screening criteria (mm/s)	Evaluation	Exceeding pipe section
1	x	5.7			
	y	4.1		Ok	
	z	1.5			
2	x	7.4			
	y	6.8		Ok	
	z	4.6			
3	x	9.6			
	y	5.0	14.8	Ok	
	z	3.0			
4	x	9.5			
	y	4.9		Ok	
	z	13.5			
5	x	10.3			
	y	5.3		NG	
	z	15.0			
6	x	6.0			
	y	5.4		Ok	
	z	3.1			
7	x	12.1			
	y	42.2		NG	
	z	4.3			
8	x	11.9			
	y	18.2		NG	
	z	15.2			
9	x	19.9	17.2		
	y	18.1		NG	
	z	16.3			
10	x	3.4			
	y	20.4		NG	
	z	19.7			
11	x	3.4			
	y	2.0		Ok	
	z	1.4			

dynamic absorber is at a level that facilitates displacement; thus, there is no issue concerning cold joints, and it can be installed while maintaining the deformed shape and controlling the vibration while operating the facility. Similarly, the viscous damper enables static displacement and selectively controls only dynamic displacement; hence, there is no concern about thermal stress. Therefore, damping was controlled for the displacement control of a particular section, and dynamic absorbers and viscous dampers were installed for the optimal vibration reduction.
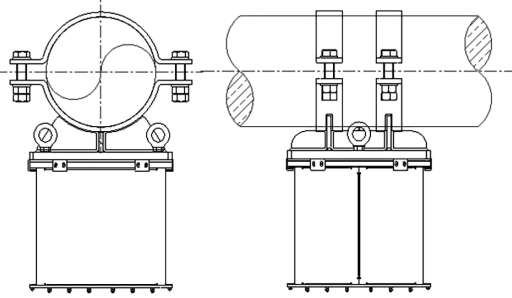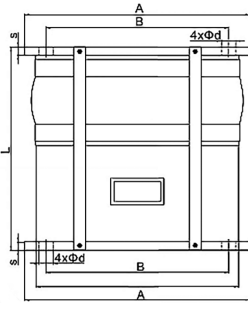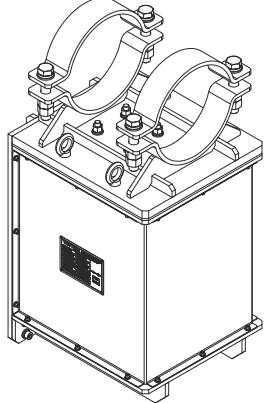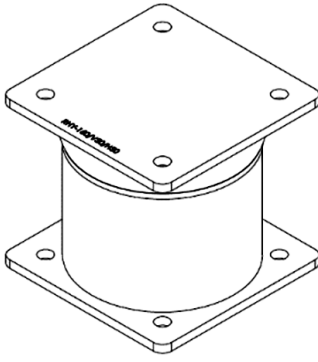
3.1. Dynamic absorber and viscous damper

The dynamic absorber in Table 3 is used when the vibration level of a single frequency and a certain direction is large and when damping higher than that of the viscous damper is required. It is installed directly on the pipe, and it is advantageous in that a support frame need not be

installed because the connecting structure is not required in the surrounding structures. A vibration reduction effect is expected because it enables the occurrence of displacement, and there is no concern for cold joints. Moreover, it can be installed even during the operation of a facility because it controls vibrations while maintaining the deformed shape. However, the target frequency must be known exactly through mode analysis. Therefore, the Passive Dynamic Absorber (PDA)-70H model with a dynamic mass of 70±10 kg among PDA models with a reduced frequency range of 3 to 20 Hz was selected for this pipe system with a natural frequency of 3.25 Hz.

The viscous damper in Table 3 is used when the vibration level is large, and stress transfer to other parts is expected when reinforcing the supports. The disadvantage is that the field conditions should be considered, and installation is difficult because a frame for supporting the

Table 3. Specifications of the dynamic absorber and viscous damper

	Dynamic absorber	Viscous damper
Model no.	PDA-70H or V	RHY-160/V50/H50
Elevation		
Model image		
Installation		
Mass	70±10 kg	231 kg

damper is required. However, it has the advantage that a reduction in the entire frequency domain is feasible in contrast to dynamic absorbers. Furthermore, because it enables static displacements and selectively controls dynamic displacements, there is no concern for thermal stress, and because it facilitates vibration control while maintaining the deformed shape, it can be installed during the pipe operation. Although a computational method is used to conservatively determine the load transmitted to the frame by estimating the damper force according to the magnitude of vibration, most of the specifications of the damper, which are affected by the site installation requirements, are determined based on the diameter of the pipe. Therefore, the Rotary Hydraulic Damper (RHY)-160/V50/H50 model was selected for this pipe system to be installed on the 24-inch upper pipe.

3.2. Application of vibration reduction measures

This paper proposes a model for evaluating and controlling vibration levels in an operating oil refinery piping system, which is composed of three steps outlined in a flowchart in Figure 7. In the design step, proposed attachment locations for accelerometers are determined based on field survey, steel pipe inspections and document reviews. The accelerometers are placed primarily at points where vibration intensity is highest, with a total of 11 attachment points selected in this study, including the branching point, elbow, and support of the piping system (Figure 4). Next in the evaluation step vibration was measured using accelerometers, and the vibration velocity baseline was calculated and compared according to the ASME OM Part 3 (ASME, 2001) correction factor calculated using the pipe material, diameter, and boundary conditions to determine which intervals were exceeded. The pipes were diagnosed according to the given velocity baseline, and the vibration reduction was examined by applying and installing appropriate reduction measures in the exceeding sections, considering the vibration sources and field installation conditions, and targeting the frequency reduction domain.

The dynamic absorber was installed in the lower section (point 7) of the pipeline shown in Figure 4. Vibration in the horizontal direction, at a frequency of 3.25 Hz, occurred dominantly in the pipe, and the section was located at a height at which the steel frame could not be constructed. Therefore, we devised a method for installing two dynamic absorbers that can operate effectively at a single frequency to control the vibration.

Viscous dampers were installed in the upper section of the pipeline (points 9 and 10) shown in Figure 4. Because vibrations occurred in symmetry at the uppermost and lower parts of the pipeline, it was desirable to consider vibration reduction by installing viscous dampers of two units of RHY-160/V50/H50 at the vertical support and lowermost sections. They were installed to prevent interference from the existing spring support and guide support.
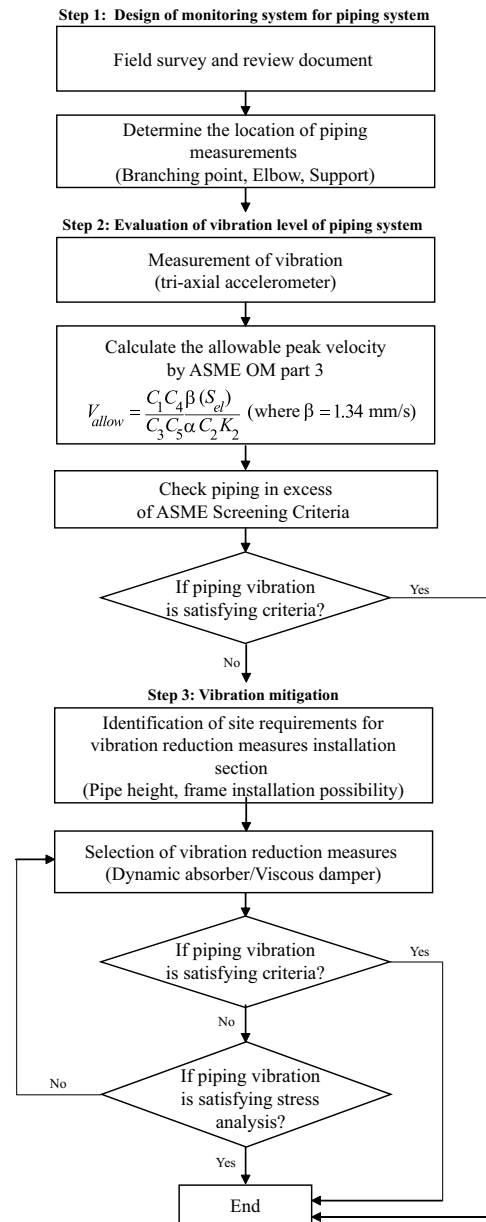

Figure 7. Flow chart of monitoring system for the vibration of the piping system

The interconnected nature of refinery pipelines implies that vibrations at one point strongly affect those at adjacent points. For points 5, 7, 8, 9, and 10, the most cost-effective and efficient approach involves mitigating vibrations on both sides of a target structure when they exceed the baseline, yielding collateral central vibration reduction. This eliminates the need for ubiquitously attaching vibration reduction devices. In light of site conditions, priority was assigned to point 7 due to its remote location without support, coupled with an independent Y-direction vibration mode, resulting in the highest peak velocity. Consequently, our strategy included floating point 8 and installing vibration reduction devices at points 9 and 10. As outlined in Section 2.2, the ASME screening criteria establish a velocity range of 14.8–32.6 mm/s for a 10-inch pipe. The recorded peak velocity at point 5 reached

15.0 mm/s, only slightly above the baseline's most conservative value of 14.8 mm/s. The reduction in vibrations following the installation of vibration reduction devices at points 7, 9, and 10 also extends to point 5. Attaching a vibration reduction device to point 5, with its marginal exceedance of the conservative velocity threshold, becomes unnecessary. Therefore, considering the extent of ASME standard exceedance, structural characteristics of oil pipelines, and site conditions, vibration reduction devices were not affixed at points 5 and 8.

4. Comparison of vibration levels before and after installation of dampers and absorber

Dynamic absorbers were installed at point 7, and viscous dampers were installed at points 9 and 10. The vibration responses and frequencies at the points before and after installation were measured and compared (Figure 8). As shown in Figure 8, the vibration responses decreased at points 7, 9, and 10. The reduction rates of the vibrations for points 7, 9, and 10 were approximately 52%, 70%, and 79%, respectively. The global response reduction characteristics of the viscous damper installed at points 9 and 10 and the local response reduction characteristics of the dy-

namic absorber installed at point 7 are shown in Figure 8.

In actual field measurement results, the vibration response, which was large at 3.5 Hz before the installation of passive dynamic absorbers (PDAs), decreased after PDA installation and tuning because the response frequency was divided into 3 and 4 Hz, similar to the change in ideal vibration data (Figure 8a).

Although the PDA has less vibration reduction effect per unit product than the viscous damper, it exhibits an excellent vibration reduction effect at high positions of vibration at which installation of the structure is impossible, as for the pipes in this study.

The combined measurement value in Table 4 represents the square root of the sum of the squares (SRSS) value of the vibration values in each direction and is the maximum vibration amplitude value in all directions during the measurement time. The combined measurement values in Table 4 represent the square root of the sum of the squares (SRSS) of x, y, and z directions at the same time during the total measurement time. In contrast, the vibration measurement values represent the peak values during the total measurement time. Thus, the combined measurement value can be equal to or larger than the maximum value in each direction but not smaller.
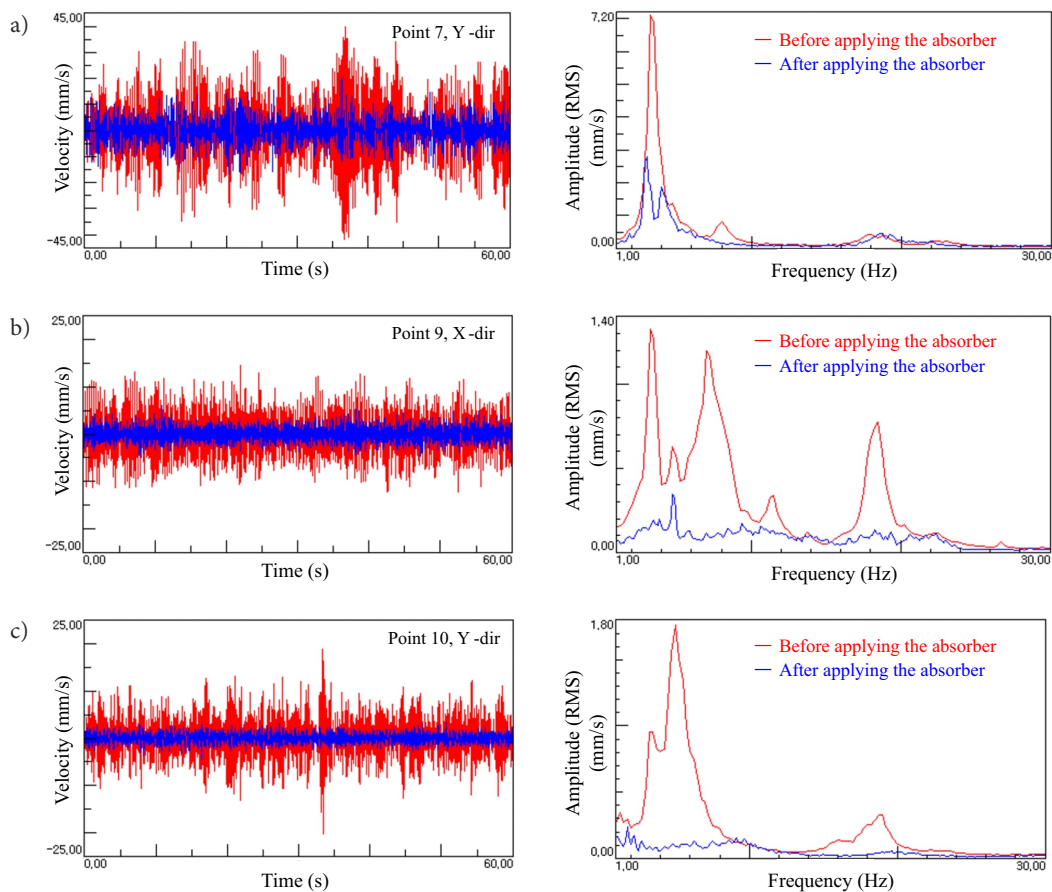
Figure 8. Velocity (left column) and frequency (right column) measured at points 7, 9, and 10 before and after installation of the absorber and damper: a – Velocity and frequency measured at point 7 (Y-dir) before and after installation of the absorber; b – Velocity and frequency measured at point 9 (X-dir) before and after installation of the damper; c – Velocity and frequency measured at point 10 (Y-dir) before and after installation of the damper

Table 4. Evaluation results of ASME screening criteria

Measurement point (Node no.)		Vibration measurement value		Screening criteria (mm/s)	Evaluation	Combined measurement value		Reduction rate (%)
		Before installation (mm/s)	After installation (mm/s)			Before installation (mm/s)	After installation (mm/s)	
7	x	12.1	4.1	17.2	NG	42.2	20.2	52.2
	y	42.2	20.2					
	z	4.3	4.4					
8	x	11.9	–		Not measured	–	–	–
	y	18.2	–					
	z	15.2	–					
9	x	19.9	6.1		Ok	20.9	6.2	70
	y	18.1	4.0					
	z	16.3	3.0					
10	x	3.4	2.3		Ok	22.2	4.7	79
	y	20.4	4.7					
	z	19.7	3.4					

Table 5. Fatigue stress evaluation for steel pipes

Point	Stress (M/Z)	C_2K_2	S_{alt}	S_{el}/α	Result
7	12.95	3.3	42.74	53	Ok
9	8.01	3.3	26.43		Ok
10	5.07	3.3	16.73		Ok

In the pipe vibration evaluation results based on the ASME screening criteria, the measurement result exceeded the baseline at point 7 on the pipe after applying the measures; however, the other two points satisfied the baseline. At points 9 and 10, the vibration reduction rates were approximately 70% and 79%, respectively. The peak velocity in the y-direction at point 7 was 42.2 mm/s before installing the absorber. This surpassed the entire range of the screening criteria (14.8–32.6 mm/s) and was reduced to 20.2 mm/s after reinforcement, falling within the criteria. While 20.2 mm/s falls within the acceptable range of 14.8–32.6 mm/s, it exceeds the most stringent criterion of 14.8 mm/s suggested in this paper. Therefore, asserting that a safe vibration level is achieved based on this is incomplete. Therefore, the conformity with the vibration criterion was further evaluated using stress evaluation based on Eqn (4). The stress evaluation result confirmed that the vibration criteria were satisfied in all sections, including point 7, as shown in Table 5.

Conclusions

To control the vibration of the piping in an oil refinery, appropriate vibration reduction countermeasures have been selected after analyzing the site requirements such as the vibration source and material, size, and frame installation possible. Vibration data was obtained from the acceleration response of an accelerometer installed at 11 points of two types of bends of oil refinery pipelines with different

pipe directions and sizes, and the measured vibration level was compared with the allowable vibration level according to the ASME OM part 3 standard.

In the velocity measurement, it has been observed that the vibration levels of five of the 11 measurement points exceeded the allowable vibration level. After comparing the measured and allowable vibrations, two types of vibration reduction measures, i.e., dynamic absorbers and viscous dampers, were considered to reduce the vibration level. For the effective vibration mitigation strategies of the pipe system, vibration reduction devices were not installed at point 5, which slightly exceeds the ASME standard, and at point 8, where potential secondary mitigation effects could be achieved.

After installing the vibration reduction measures, the vibration responses reduced by 52%, 70%, and 79%, respectively, at the aforementioned three points. The responses of the frequency component also exhibited local and global reductions of approximately 50–80% at each point after the installation of dynamic absorbers and viscous dampers.

The proposed method determines sections of the pipe system that exceed the standard by measuring only the acceleration in the operating state of the installed pipe system, evaluates the safety, and proposes a method of adopting an appropriate damping reinforcement device considering the site requirements for the identified sections. It is demonstrated that the safety of the pipe system in operation can be diagnosed and a vibration reduction countermeasure can be selected without complicated and unreliable flow analysis at the design stage.

Author contributions

Sang Geun Bae contributed to the experimental design, Data collection and Analysis, Evaluation of system, writing and revising the manuscript. Jewoo Choi contributed to the Data collection and Analysis, Evaluation of system. Deok Shin Kang contributed to the Field support and assistance. Taehoon Hong Kang contributed to the revision and analysis. Dong-Eun Lee contributed to the revision and analysis of the system. The corresponding author Hyo Seon Park contributed to the conceptualization of the study, Data analysis and interpretation, and manuscript writing.

Disclosure statement

The authors declare no conflict of interest.

References

Al-Obaidi, A. R. (2020). Detection of cavitation phenomenon within a centrifugal pump based on vibration analysis technique in both time and frequency domains. *Experimental Techniques*, 44, 329–347. https://doi.org/10.1007/s40799-020-00362-z

American Society of Mechanical Engineers. (2001). *Requirements for preoperational and initial start-up vibration testing of nuclear power plant piping systems* (ASME OM3).

American Society of Mechanical Engineers. (2010). *Boiler & pressure vessel code section III, division 1: Mandatory appendix I*.

American Society of Mechanical Engineers. (2012). *Operation and maintenance of nuclear power plants, Division 2: OM standards contents – Part 3: Vibration testing of piping systems. Nonmandatory appendix D, velocity criterion*.

Amezquita-Sanchez, J. P., & Adeli, H. (2016). Signal processing techniques for vibration-based health monitoring of smart structures. *Archives of Computational Methods in Engineering*, 23, 1–15. https://doi.org/10.1007/s11831-014-9135-7

Ariaratnam, S. T., & Namachchivaya, N. S. (1986). Dynamic stability of pipes conveying pulsating fluid. *Journal of Sound and Vibration*, 107, 215–230. https://doi.org/10.1016/0022-460X(86)90233-6

Bhandari, S., & Jotautienė, E. (2022). Vibration analysis of a roller bearing condition used in a tangential threshing drum of a combine harvester for the smooth and continuous performance of agricultural crop carvesting. *Agriculture*, 12(11), 1969. https://doi.org/10.3390/agriculture12111969

Brunesi, E., Nascimbene, R., Pagani, M., & Beilic, D. (2015). Seismic performance of storage steel tanks during the May 2012 Emilia, Italy, earthquakes. *Journal of Performance of Constructed Facilities*, 29(5), 04014137. https://doi.org/10.1061/(ASCE)CF.1943-5509.0000628

Chock, G. (2006). *Preliminary observations on the Hawaii earthquakes of October 15*.

Escaler, X., Egusquiza, E., Farhat, M., Avellan, F., & Coussirat, M. (2006). Detection of cavitation in hydraulic turbines. *Mechanical Systems and Signal Processing*, 20(4), 983–1007. https://doi.org/10.1016/j.ymssp.2004.08.006

Gabbianelli, G., Perrone, D., Nascimbene, R., & Paolacci, F. (2022). Seismic vulnerability assessment and fragility functions derivation for steel storage legged tanks. In *Pressure Vessels and Piping Conference* (Vol. 86199). American Society of Mechanical Engineers. https://doi.org/10.1115/PVP2022-84416

Gabbianelli, G., Milanesi, R. R., Gandelli, E., Dubini, P., & Nascimbene, R. (2023). Seismic vulnerability assessment of steel storage tanks protected through sliding isolators. *Earthquake Engineering* & *Structural Dynamics*, 52(9), 2597–2618. https://doi.org/10.1002/eqe.3885

González, E., Almazán, J., Beltrán, J., Herrera, R., & Sandoval, V. (2010). Performance of stainless steel winery tanks during the 02/27/2010 Maule Earthquake. *Engineering Structures*, 56, 1402–1418. https://doi.org/10.1016/j.engstruct.2013.07.017

Guo, Y. Q., Zhang, H. Q., Wang, Y. N., & Dai, J. (2022). Research on seismic acceleration waveform reproduction based on time-frequency hybrid integration algorithm. *IEEE Access*, 10, 94887–94897. https://doi.org/10.1109/ACCESS.2022.3202969

Hussein, D. S., & Al-Waily, M. (2019). Active vibration control analysis of pipes conveying fluid rested on different supports using state-space method. *International Journal of Energy and Environment*, 10, 329–344.

Iqbala, H., Tesfamariama, S., Haiderb, H., & Sadiqa, R. (2017). Inspection and maintenance of oil & gas pipelines: A review of policies. *Structure and Infrastructure Engineering*, 13, 794–815. https://doi.org/10.1080/15732479.2016.1187632

Jweeg, M. J., & Ntayeesh, T. J. (2015). Active vibration control analysis of cantilever pipe conveying fluid using smart material. *Innovative Systems Design and Engineering*, 6, 53–79.

Kabir, G., Sadiq, R., & Tesfamariam, S. (2016). A fuzzy Bayesian belief network for safety assessment of oil and gas pipelines. *Structure and Infrastructure Engineering*, 12(8), 874–889. https://doi.org/10.1080/15732479.2015.1053093

Kim, D., Oh, B. K., Park, H. S., Shim, H., & Kim, J. (2017). Modal identification for high-rise building structures using orthogonality of filtered response vectors. *Computer-Aided Civil and Infrastructure Engineering*, 32, 1064–1084. https://doi.org/10.1111/mice.12310

Miranda, E., Mosqueda, G., Retamales, R., & Pekcan, G. (2010). Performance of nonstructural components during the 27 February 2010 Chile earthquake. *Earthquake Spectra*, 28, 453–471. https://doi.org/10.1193/1.4000032

Miwa, S., Mori, M., & Hibiki, T. (2015). Two-phase flow induced vibration in piping systems. *Progress in Nuclear Energy*, 78, 270–284. https://doi.org/10.1016/j.pnucene.2014.10.003

Mossa, N. F., Shareef, W. F., & Shareef, F. F. (2018). Design of oil pipeline monitoring system based on wireless sensor network Iraqi. *Iraqi Journal of Computers, Communications, Control* & *Systems Engineering*, 18, 53–62. https://doi.org/10.33103/uot.ijccce.18.2.5

Olson, L. G., & Jamison, D. (1997). Application of a general purpose finite element method to elastic pipes conveying fluid. *Journal of Fluids and Structures*, 11(2), 207–222. https://doi.org/10.1006/jfls.1996.0073

Ozdemir, Z., Souli, M., & Fahjan, Y. (2010). Application of nonlinear fluid-structure interaction methods to seismic analysis of anchored and unanchored tanks. *Engineering Structures*, 32(2), 409–423. https://doi.org/10.1016/j.engstruct.2009.10.004

Park, H. S., & Oh, B. K. (2018). Real-time structural health monitoring of a supertall building under construction based on visual modal identification strategy. *Automation in Construction*, 85, 273–289. https://doi.org/10.1016/j.autcon.2017.10.025

Parvizsedghy, L., Senouci, A., Zayed, T., & Mirahadi, S. F. (2015). Condition-based maintenance decision support system for oil and gas pipelines. *Structure and Infrastructure Engineering*, *11*(10), 1323–1337. https://doi.org/10.1080/15732479.2014.964266

Riveiro, B., DeJong, M. J., & Conde, B. (2016). Automated processing of large point clouds for structural health monitoring of masonry arch bridges. *Automation in Construction*, *72*, 258–268. https://doi.org/10.1016/j.autcon.2016.02.009

Senouci, A., Elabbasy, M., Elwakil, E., Abdrabou, B., & Zayed, T. (2014). A model for predicting failure of oil pipelines. *Structure and Infrastructure Engineering*, *10*, 375–387. https://doi.org/10.1080/15732479.2012.756918

Seo, Y. S., Jeong, W. B., Yoo, W. S., & Jeong, H. K. (2005). Frequency response analysis of cylindrical shells conveying fluid using finite element method. *Journal of Mechanical Science and Technology*, *19*, 625–633. https://doi.org/10.1007/BF02916184

Sepehry, N., Ehsani, M., Zhu, W., & Bakhtiari-Nejad, F. (2020). Application of scaled boundary finite element method for vibration-based structural health monitoring of breathing cracks. *Journal of Vibration and Control*, *27*(23–24), 2870–2886. https://doi.org/10.1177/1077546320968646

Sun, Y., Gu, Y., & Xiong, H. (2013). Studied and their application of vibration control technologies. *International Journal of Computer Science Issues*, *10*(2), 311–318.

Taghavi, S., & Miranda, M. M. (2003). *Response assessment of nonstructural building elements*. Pacific Earthquake Engineering Research Center.

Tan, J., Ho, M., Zhang, S. C., & Jiang, P. (2019). Experimental study on vibration control of suspended piping system by single-sided pounding tuned mass damper. *Applied Sciences*, *9*(2), 285. https://doi.org/10.3390/app9020285

Valentín, D., Presas, A., Valero, C., Egusquiza, M., & Egusquiza, E. (2019). Detection of hydraulic phenomena in francis turbines with different sensors. *Sensors*, *19*(18), 4053. https://doi.org/10.3390/s19184053

Vela, M., & Nascimbene, B. E. (2019). Seismic assessment of an industrial frame-tank system: development of fragility functions. *Bulletin of Earthquake Engineering*, *17*, 2569–2602. https://doi.org/10.1007/s10518-018-00548-2

Wang, S., Ren, Q., & Qiao, P. (2006). Structural damage detection using local damage factor. *Journal of Vibration and Control*, *12*, 955–973. https://doi.org/10.1177/1077546306068286

Wang, J., Zhao, J., Liu, Y., & Shan, J. (2021). Vision-based displacement and joint rotation tracking of frame structure using feature mix with single consumer-grade camera. *Structural Control and Health Monitoring*, *28*(12), e2832. https://doi.org/10.1002/stc.2832

Whittaker, A. S., & Soong, T. T. (2003). An overview of nonstructural components research at three US Earthquake Engineering Research Centers. In *Proceedings of ATC Seminar on Seismic Design, Performance, and Retrofit of Nonstructural Components in Critical Facilities* (pp. 271–280).

Xiao, F., Chen, G. S., & Hulsey, Z. W. (2021). Signature extraction from the dynamic responses of a bridge subjected to a moving vehicle using complete ensemble empirical mode decomposition. *Journal of Low Frequency Noise, Vibration and Active Control*, *40*, 278–294. https://doi.org/10.1177/1461348419872878

Xue, F., Lin, L., Ti, W., & Lu, N. (2007). Vibration assessment method and engineering applications to small bore piping in nuclear power plant. In *Second International Symposium on Nuclear Power Plant Life Management*, Shanghai, China.

Yildirim, U., Oguz, O., & Bogdanovic, N. (2013). A prediction-error-based method for data transmission and damage detection in wireless sensor networks for structural health monitoring. *Journal of Vibration and Control*, *19*, 2244–2254. https://doi.org/10.1177/1077546313501538

Yun, D. Y., Kim, M., Bae, S. G., Choi, J. W., Shim, H. B., Hong, T., & Park, L. D. (2021). Field measurements for identification of modal parameters for high-rise buildings under construction or in use. *Automation in Construction*, *121*, 103446. https://doi.org/10.1016/j.autcon.2020.103446

Zhang, Y. L., Gorman, D., & Reese, J. M. (2001). A finite element method for modelling the vibration of initially tensioned thin-walled orthotropic cylindrical tubes conveying fluid. *Journal of Sound and Vibration*, *245*, 93–112. https://doi.org/10.1006/jsvi.2000.3554

Zhang, R., Cao, Y., & Dai, K. (2021). Response control of wind turbines with ungrounded tuned mass inerter system (TMIS) under wind loads. *Wind and Structures*, *32*, 573–586.

Zhou, Y. L., Maia, N. M., & Wahab, A. (2018). Damage detection using transmissibility compressed by principal component analysis enhanced with distance measure. *Journal of Vibration and Control*, *24*, 2001–2019. https://doi.org/10.1177/1077546316674544

Zhu, H., Zhou, Y., & Hu, Y. (2020). Displacement reconstruction from measured accelerations and accuracy control of integration based on a low-frequency attenuation algorithm. *Soil Dynamics and Earthquake Engineering*, *133*, 106122. https://doi.org/10.1016/j.soildyn.2020.106122